ZnO-Based Hollow Microspheres: Biopolymer-Assisted Assemblies from ZnO Nanorods

Shuyan Gao, Hongjie Zhang,* Xiaomei Wang, Ruiping Deng, Dehui Sun, and Guoli Zheng

Key Laboratory of Rare Earth Chemistry and Physics, Changchun Institute of Applied Chemistry, Chinese Academy of Sciences, and Graduate School of the Chinese Academy of Sciences, Changchun 130022, P. R. China

Received: May 10, 2006; In Final Form: June 9, 2006

Many efforts have been made in fabricating three-dimensional (3D) ordered zinc oxide (ZnO) nanostructures due to their growing applications in separations, sensors, catalysis, bioscience, and photonics. Here, we developed a new synthetic route to 3D ZnO-based hollow microspheres by a facile solution-based method through a water-soluble biopolymer (sodium alginate) assisted assembly from ZnO nanorods. The products were characterized by X-ray diffraction, field emission scanning electron microscopy, transmission electron microscopy, selected area electron diffraction, and X-ray photoelectron spectroscopy. Raman and photoluminescence spectra of the ZnO-based hollow microspheres were obtained at room temperature to investigate their optical properties. The hollow microspheres exhibit exciting emission features with a wide band covering nearly all the visible region. The calculated CIE (Commission Internationale d'Eclairage) coordinates are 0.24 and 0.31, which fall at the edge of the white region (the 1931 CIE diagram). A possible growth mechanism of the 3D ZnO superstructures based on typical biopolymer−crystal interactions in aqueous solution is tentatively proposed, which might be really interesting because of the participation of the biopolymer. The results show that this biopolymer-directed crystal growth and mediated self-assembly of nanocrystals may provide promising routes to rational synthesis of various ordered inorganic and inorganic−organic hybrid materials with complex form and structural specialization.

Introduction

Zinc oxide (ZnO), an important II−VI semiconductor with a direct wide band gap (3.37 eV) and a large exciton binding energy (60 meV), has become one of the key technological materials and of considerable interest due to its wide applications ranging from surface acoustic wave filters,[1] photovoltaic[2] and optoelectronic devices,[3] sensors,[4] varistors,[5] (photo)catalysis,[6] light-emitting diodes,[7] photodetectors,[8] optical modulator waveguides,[9] and solar cells,[10] together with its biosafety and biocompatibility.[11] Therefore, we have witnessed growing efforts toward synthesizing various ZnO nanostructures such as nanobelts,[12] nanowires,[13] nanotubes,[14] nanoribbons,[15] nanopins,[16] nanocables,[14a] nanorods,[14d,17] and nanoneedles[18] over the past decades. The aesthetic morphologies, wide band gap, and strong exciton binding energy have triggered great interest in ZnO-based nanoscience and nanotechnology, thus motivating great progress in developing various routes (including vapor−liquid−solid growth, thermal evaporation, thermal decomposition, electrochemical deposition, and solution-phase processes) to tailor the morphology and size for the purpose of obtaining better properties or for applying them to practical use.[19] Of these methods, the facile solution procedures may be the most simple and effective way to prepare well-crystallized materials at a relatively low temperature. Moreover, the advantages of solution-based methods have also involved the remarkable influence of organic additives on the size and morphology of the final products.[20]

Many of the previously reported synthetic methods are limited to the formation of the preferred one-dimensional (1D) ZnO nanostructure, due to its highly anisotropic growth rate along the *c* axis. Their self-assembly into 2D and 3D ordered superstructures are urgently needed to meet the demand for exploring the potentials of ZnO.[20] In fact, different 1D, 2D, and 3D nanostructures have been fabricated by several self-assembly processes based on different driving mechanisms.[20,21] However, compared with this great success in the spatial orientation of nanocrystals, little attention has been devoted to the controlled organization of primary building units into 3D curved nanostructures. Furthermore, fine control of curved nanostructures is relatively difficult due to the lack of understanding of the formation mechanism, which hinders the development of secondary organization of subunits. From this point of view, more investigation of the fabrication methods and systematic research on the formation mechanism are highly desired for controlling the growth of complex nanostructures. Though the curved nanostructures have recently been reported,[22] more

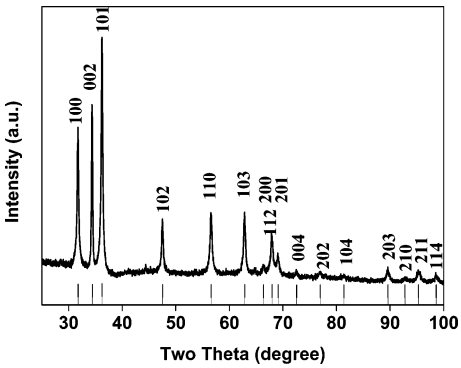

Figure 1. XRD patterns of hollow ZnO microspheres. The vertical lines represent the data of JCPDS card no. 36-1451.

* Corresponding author. Telephone: +86−431−5262127. Fax: +86−431−5698041. E-mail: hongjie@ciac.jl.cn.

10.1021/jp062850s CCC: $33.50
Published on Web 07/22/2006

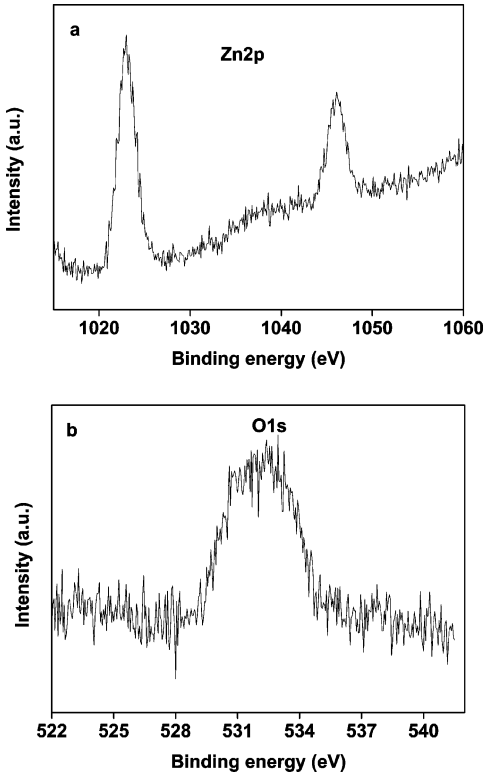

Figure 2. XPS spectra of the hollow ZnO microspheres.

effective methods via the simple routes are still required. Here, we developed a low-temperature and environmentally benign solution-phase approach to fabricate 3D ZnO-based hollow microspheres in the presence of water-soluble biopolymer (sodium alginate, SA). The hollow microspheres exhibit exciting emission features with wide band covering nearly all the visible region. The calculated CIE (Commission Internationale d'Eclairage) coordinates are 0.24 and 0.31, which fall at the edge of the white region (the 1931 CIE diagram).[23] The present work verifies that it is possible to directly grow curved, 3D-ordered assemblies built from 1D semiconductor nanocrystals through a one-step aqueous solution-phase chemical route at low temperature. A possible growth mechanism of the ZnO nanostructures based on typical biopolymer−crystal interactions in aqueous solution is tentatively proposed.

Experimental Section

All chemicals were used as received. SA was purchased from Acros, while all other chemicals were supplied by Beijing Chemicals Co. Ltd. To prepare hollow ZnO microspheres, 0.55 mL of a 25.4 mM aqueous solution of SA (calculated by the repeating unit) was added to 30 mL of deionized water containing 1.5 mmol $Zn(Ac)_2 \cdot 2H_2O$. Then 0.9 mL of 28 wt % commercial ammonia was added dropwise under constant stirring. The final pH value was 10.38. The resulting mixtures were transferred into a 50 mL Teflon-lined autoclave and heated at 100 °C for 7 h. White powders collected after reaction were washed with DMSO and deionized water.

The phase and purity of the product was determined by powder X-ray diffraction (XRD), using a Rigaku D/Max 2500 V/PC X-ray diffractometer equipped with high-intensity Cu $K\alpha_1$ radiation ($\lambda = 1.54056$ Å). The morphology, size, and composition of the sample were examined by field emission scanning electron microscopy (FESEM, an XL30 ESEM FEG scanning

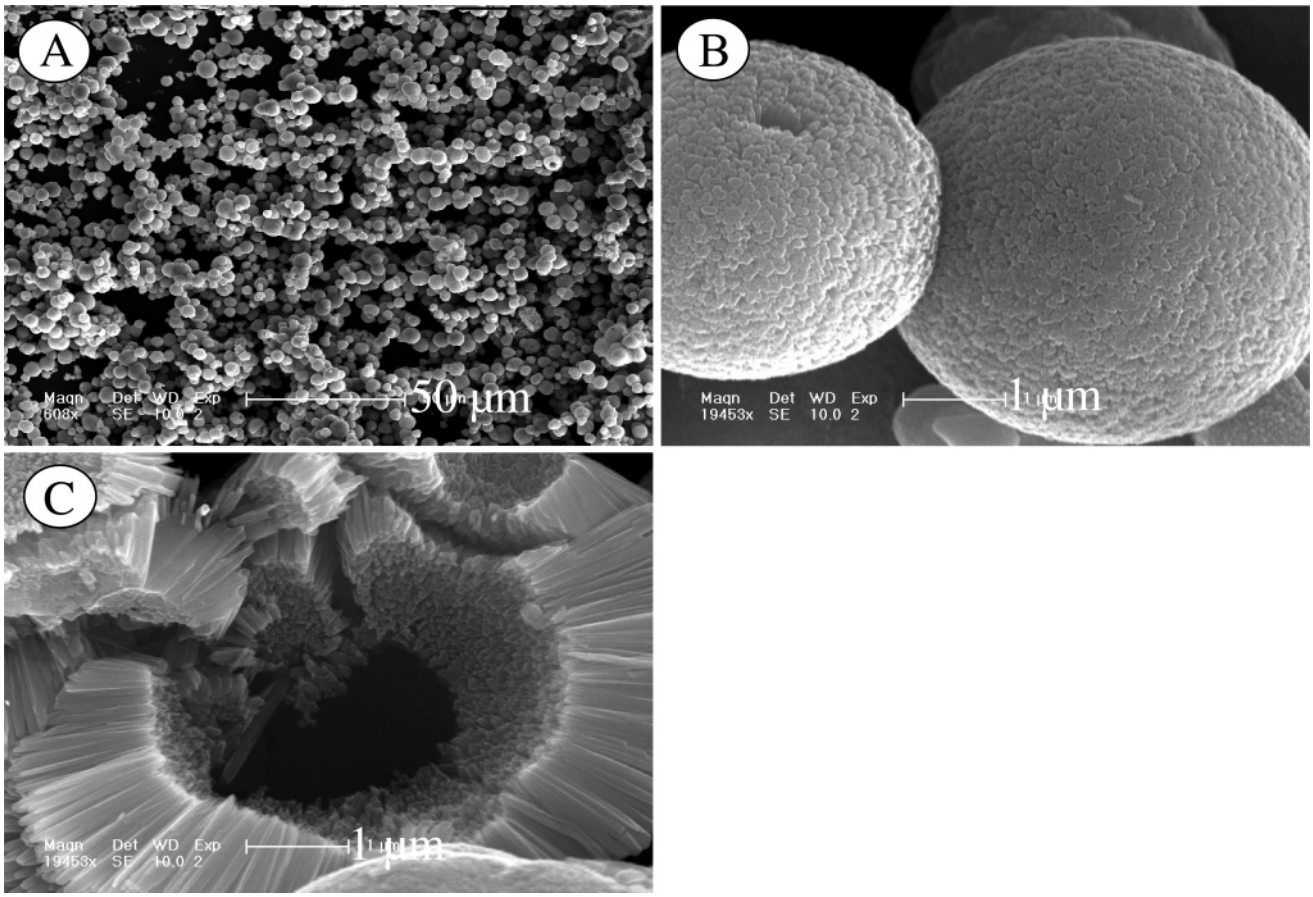

Figure 3. FESEM images of the ZnO microspheres: (A) low-magnification image, (B) high-magnification image, and (C) the central part of the microspheres.

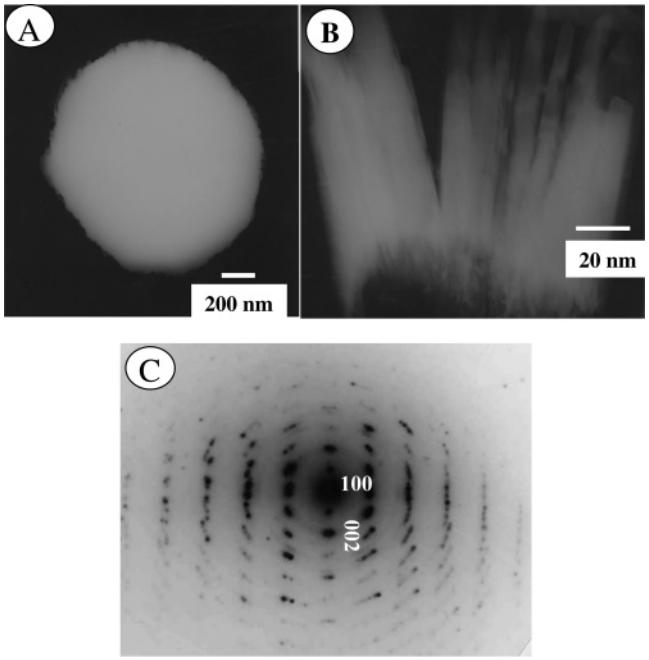

Figure 4. TEM images of the hollow ZnO microspheres: (A) a single microsphere, (B) the subunit ZnO nanorods, and (C) the SAED pattern.

electron microscopy operated at 20 kV). The structure of the product was investigated by transmission electron microscopy (TEM) and selected area electron diffraction (SAED) (JEM JEOL 2010, accelerating voltage 200 kV). The room-temperature photoluminescence (PL) measurement was carried out on an F-4500 spectrophotometer using the 325-nm excitation line of Xe light. Raman spectra were recorded on a Raman 960 FT-Raman spectrometer using a laser beam with an excitation wavelength of 1064 nm and a resolution of 8 cm^{-1}. X-ray photoelectron spectroscopy (XPS) was collected on an ESCALab MKII X-ray photoelectron spectrometer, using nonmonochromatized Mg Kα X-ray as excitation source.

Results and Discussions

Biopolymer-controlled crystallization of ZnO crystals was carried out in aqueous solution under hydrothermal condition. The phase purity of the product obtained in the presence of SA was examined by XRD, which is depicted in Figure 1. All diffraction peaks can be readily indexed to the hexagonal phase (space group $P6_3mc$) of ZnO, with a unique polar axis parallel to the *c*-axis and calculated cell parameters $a = 3.25$ and $c = 5.21$ Å. With the presence of SA, we found that there is an increase of intensity of the (002) crystallographic plane after comparing the relative intensities with those from JCPDS card no. 36-1451, which indicates a preferential growth along the *c* axis. To obtain chemical states of the elements within the samples, we performed detailed analysis of XPS spectra. The binding energies were corrected for specimen charging by calibrating the C1s peak to 284.6 eV. Figure 2, parts a and b, depicts the XPS spectra of Zn2p and O1s, respectively. The binding energies of both $Zn2p_{1/2}$ (1046 eV) and $Zn2p_{3/2}$ (1023 eV) are slightly larger than the values (1045 and 1022 eV) of Zn in the bulk ZnO. This indicates that Zn is in the +2 valence state within an oxygen-deficient environment.[24]

Low-magnification FESEM observations show that the panoramic morphology of the as-obtained ZnO product is mainly composed of uniform, spheric architectures ranging from 3 to 5 μm in diameter (Figure 3A). Closer observations (Figure 3B) show that the surface of the architecture is not smooth.

SCHEME 1: Schematic Illustration of the Proposed Formation Mechanism for the as-Obtained Hollow Microsphere Superstructures under Typical Synthetic Conditions[a]

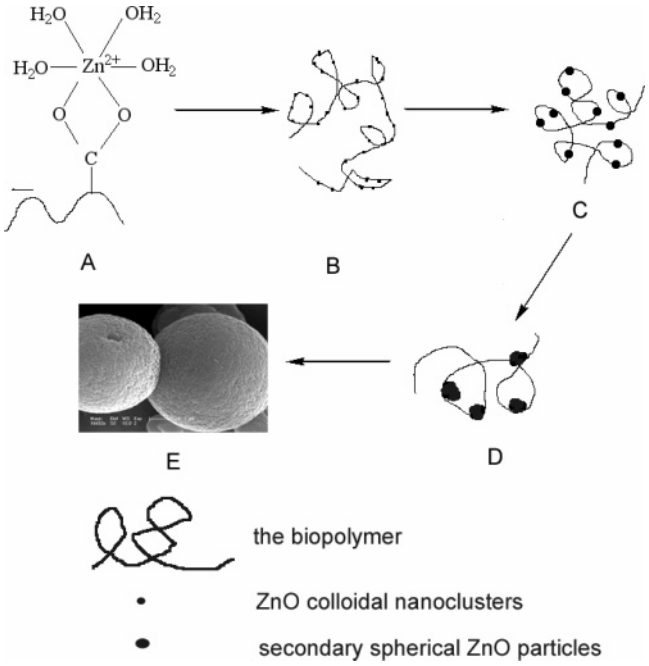

[a] (A) the electrostatic attraction between the positively charged Zn^{2+}−water complex and the carboxylic groups of the negatively charged SA; (B) SA-stabilized ZnO colloidal nanoclusters; (C) formation of secondary spherical particles; (D) coagulation of secondary spherical particles into large particles; (E) formation of nanorod-based shells at the cost of the small nanoclusters in the system.

Furthermore, there might be some pores presented on such a surface. The examination of an intermediate (Figure 3C) vividly reveal that the structure of these spheric architectures is built from a single layer of radially oriented nanorods with average diameter of ca. 100 nm and length of 1−1.5 μm, self-wrapping to form hollow interiors 3−5 μm in outer diameter. It is worth noting that all the constituent nanorods are radially aligned with their growth axes perpendicular to the surface of the microspheres without any substrate support. EDS microanalysis clearly shows that the Zn/O molar ratio of Zn and O elements in the sample is ca. 1:1.

Figure 4A shows a typical TEM image of an isolated ZnO-nanorod-based microstructure. The circular morphology can still be observed. The contrast between the central and fringe part of the microspheres, which is usual for smaller similar-hole nanostructure, could not be observed, probably due to the thick walls of such a microstructure. Figure 4B (an intermediate product) shows the rodlike morphology with diameter of about 100 nm and length of about 1 μm, which is consistent with the results from FESEM. The SAED pattern (Figure 4C) shows that the ZnO microstructures are well-crystallized, although they were produced at a relatively low temperature (100 °C).

As a polar crystal with hexagonal phase, ZnO is highly anisotropic and tends to grow along the *c* axis.[25] Under certain kinetic conditions, metastable 1D ZnO nanostructures can self-assemble into hierarchical structures in liquid media. The kinetic conditions could be reaction temperature, pH value of liquid media, and organic additives. We selected SA as the organic additive due to the large amount of carboxylic groups within its skeletal framework (the pK_a values of SA are 3.5 for guluronic acid and 4.0 for mannuronic acid) under alkaline

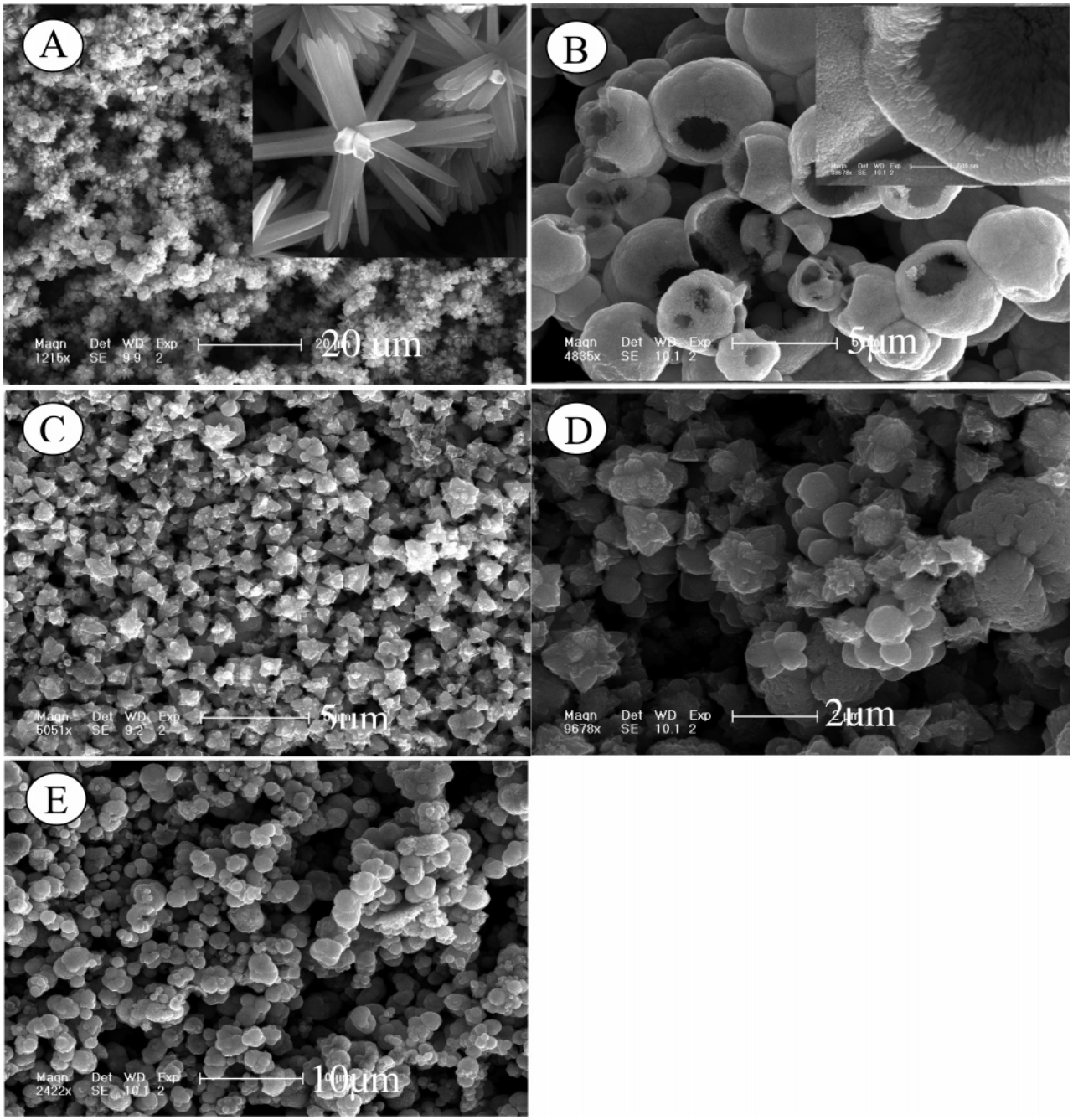

Figure 5. FESEM images of samples obtained from control experiments: (A) in the absence of SA under other identical conditions; (B) 5 times the dosage of SA under other identical conditions; (C) decreasing the pH value from 10.38 to 9.96; and increasing the pH value from 10.38 to 10.48 (D) and 10.54 (E).

conditions after adding ammonia into the reaction system. For comparison, we also carried out a hydrothermal experiment without using SA as additive. Figure 5A shows the FESEM image of the products obtained without SA. The inset clearly shows that ZnO nanorods are rooted in one center and radially extended outward. As a result, there is no interior hole. On the other hand, when 5 times dosage of SA was used, another kind of hierarchical hemispheric superstructure self-assembly from ZnO nanorods was observed under FESEM (Figure 5B and the inset). These control experiments demonstrate that the presence of an appropriate amount of water-soluble SA is crucial for the formation of hollow microspheres.

We also noticed that the pH value of the solution is another critical factor for the self-assembling process. When pH value was decreased to 9.96, the product features flower-shaped structures (Figure 5C). While it was increased to 10.48 or higher, the structure turned out to be nonuniform in terms of morphology and size (Figure 5D,E).

In classical colloid chemistry, self-assembly of colloidal particle into secondary blocks with particular micrometer size and special structure and corresponding mechanism are well-known, which is based on particle aggregation.[21a,26] In our case, the SA is dispersed within liquid medium mainly as a random coil sol bearing abundant negatively charged carboxylic groups. These random coils behave as organic matrixes, binding many zinc cations. In Scheme 1, a possible mechanism is proposed. There is electrostatic attraction between the positively charged Zn^{2+}−water complex and the negatively charged carboxylic groups of SA. The introduction of ammonia changed the pH value and caused Zn^{2+} ions to hydrolyze to form precursor,

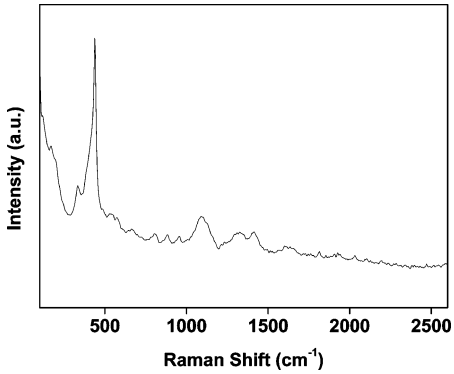

Figure 6. Room-temperature Raman spectrum of hollow ZnO microspheres.

which was still attached to SA. Upon hydrothermal treatment, the precursor decomposed and ZnO could be formed. With the process of reaction, more ZnO would be produced and may still attach to SA chains and aggregate into colloidal particles in order to minimize their surface energy. The spherical aggregates may further coagulate to form large particles.[22,27] Driven by the natural preference of polar crystal growth, ZnO tends to grow toward the exterior of the large particles, since randomly oriented growth is physically limited. This is accompanied by the energetically favorable self-assembly of tiny rods and Ostwald ripening with intermediary phases transfer from smaller nanocluster particles within the reaction system. As a result, ordered nanorod-based mesoporous shells are constructed.[22]

Raman scattering is very sensitive to the lattice microstructure. Phonon frequencies and scattering intensities determined by Raman spectroscopy can lead to conclusions concerning microscopic parameters such as bonding and structure as well as deviations from ideal crystalline counterpart.[28] ZnO belongs to the wurtzite space group. On the basis of group theory, the correlation of the site group to the factor group can be constructed as follows:

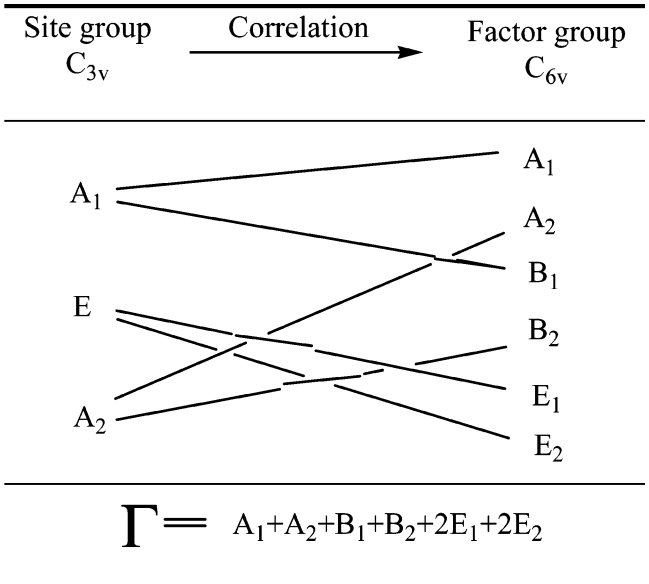

There are eight sets of optical phonon modes at the Γ point of the Brillouin zone in single-crystalline ZnO, in which the $A_1 + E_1 + 2E_2$ modes are Raman-active and expected in Raman spectra. Moreover, the A_1 and E_1 are polar and hence split into transverse optical (TO) and longitudinal optical (LO) phonon components. Figure 6 shows a typical Raman spectrum of the sample. The sharp and strong Raman peak at 438 cm^{-1} is attributed to the ZnO nonpolar optical phonons (E_2) modes,[30] which is one of the characteristic peaks of wurtzite ZnO.[31] The less prominent peak at 584 cm^{-1} corresponds to the E_1(LO) mode, which is caused by the formation of oxygen vacancies, zinc interstitials, and free carrier in ZnO[31a] and indicates that a few defects exist in the sample, which is in agreement with the XPS results. The bands at 337 and 667 cm^{-1} are assigned to A_1 second- and fourth-order overtones, respectively. All peaks and their corresponding assignments are summarized in Table 1.

TABLE 1: Raman Shift (in cm^{-1}) of the Modes Found in Raman Spectrum of the Sample and Their Assignments[61−63]

Raman shift	assignment	process	ref 29a	ref 29b	ref 29c
337	$2A_1$	acoust overtone	331		
392	A_1(TO)	first process	383	381	397
428	E_1(TO)	first process	410	407	426
439	E_2	first process	438	441	449
543	A_1(LO)	first process	540		559
584	E_1(LO)	first process	584	583	577
667	$4A_1$	acoust overtone	660		
805	$2E_1$	opt. overtone			
883	$2E_2$	acoust overtone			
1090	A_1(LO)	opt. overtone			
1326	$3E_2$	acoust overtone			
1413	$2A_1$(LO) + A_1(337)	opt. comb.			
1629	$3A_1$(LO)	opt. overtone			

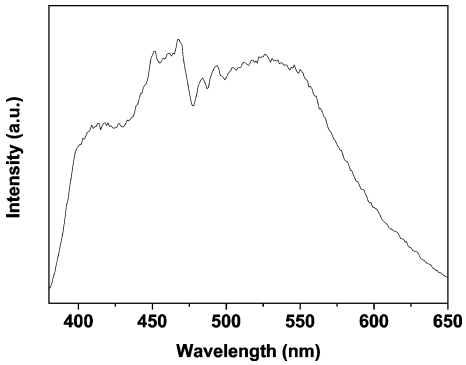

Figure 7. Room-temperature emission spectrum of hollow ZnO microspheres.

We further carried out room-temperature PL measurement of the products. As shown in Figure 7, the emission spectrum shows wide band emission covering the blue and green regions. The calculated CIE coordinates are 0.24 and 0.31, which fall at the edge of the white region (the 1931 CIE diagram).[23] It is generally accepted that the green emission results from the recombination of a photogenerated hole with a singly ionized charge state of the specific defect.[32] Thus, it is reasonable to predicate that there exist a few crystal defects in our sample. Blue emission of ZnO nanostructures, including ZnO nanotubes,[33] ZnO clusters inside mesoporous silica,[34] and ZnO nanorods[35] has been observed in previous reports. However, the origin of this emission still remains unclear, although it was speculated to be related to the radiative defects at the interface of the components of ZnO microspheres or the existence of interstitial zinc in ZnO lattices.[34] The emission spectrum obtained here is dramatically different from those of the products synthesized under different conditions,[35,36] verifying that the optical properties of ZnO crystals are very sensitive to the preparation conditions.

Conclusion

In summary, we have demonstrated a facile one-step solution-based self-assembly route for the creation of 3D hollow ZnO microspheres constructed from 1D ZnO nanorods. This makes the integration of some simple nanostructures (single function available) into a functional device and a complex system possible and provides an opportunity to investigate the formation mechanism of complex nanostructures by simple building blocks. The as-created ZnO superstructural assembilies can be used to explore the effects of spatial orientation and the arrangement of nanoscale building blocks on their collective sensing, catalytic, optical, electronic, optoelectronic, and piezoelectric properties. Such a technique might be extended to the assembling of other materials based on nanoscale building blocks. The wide band emission of the hollow ZnO microspheres suggests that such a superstructure might serve as a potential host for white-light-emitting materials.

Acknowledgment. The authors are grateful to the reviewers for their fruitful suggestions and the National Natural Science Foundation of China (Grant Nos. 20372060, 20340420326, and 20490210) and the MOST of China ("973" Program, Grant No. 2006CB601103) for continuing financial support.

References and Notes

(1) Emanetoglu, N. W.; Gorla, C.; Liu, Y.; Liang, S.; Lu, Y. *Mater. Sci. Semicond. Process.* **1999**, *2*, 247.

(2) (a) Rensmo, H.; Keis, K.; Lindstrom, H.; Sodergren, S.; Solbrand, A.; Hagfeldt, A.; Lindquist, S.-E.; Wang, L. N.; Muhammed, M. *J. Phys. Chem. B* **1997**, *101*, 2598. (b) Bauer, C.; Boschloo, G.; Mukhtar, E.; Hagfeldt, A. *J. Phys. Chem. B* **2001**, *105*, 5585.

(3) (a) Johnson, J. C.; Yan, H.; Schaller, R. D.; Haber, L. H.; Saykally, R. J., Yang, P. *J. Phys. Chem. B* **2001**, *105*, 11387. (b) Huang, M. H.; Mao, S.; Feick, H.; Yan, H.; Wu, Y.; Kind, H.; Weber, R.; Russo, R.; Yang, P. *Science* **2001**, *292*, 1897. (c) Klimov, V. I.; Mikhailovski, A. A.; McBranch, D. W.; Leatherdale, C. A.; Bawendi, M. G. *Science* **2000**, *287*, 1011. (d) Klimov, V. I.; Mikhailovski, A. A.; Xu, S.; Malko, A.; Hollingsworth, J. A.; Leatherdale, C. A.; Eisler, H.-J.; Bawendi, M. G. *Science* **2000**, *290*, 314.

(4) (a) Chadwick, A. V.; Russell, N. V.; Whitham, A. R.; Wilson, A. *Sens. Actuators, B* **1994**, *18*, 99. (b) Wang, H. T.; Kang, B. S.; Ren, F.; Tien, L. C.; Sadik, P. W.; Norton, D. P.; Pearton, S. J.; Lin, J. *Appl. Phys.* Lett. **2005**, *86*, 243503. (c) Batista, P. D.; Mulato, M. *Appl. Phys. Lett*. **2005**, *87*, 143508.

(5) (a) Gupta, T. K. *J. Am. Ceram. Soc.* **1990**, *73*, 1817. (b) Hennings, D. F. K.; Hartung, R.; Reijnrn, P. J. *J. Am. Ceram. Soc*. **1990**, *73*, 645. (c) Raghu, N.; Kutty, T. R. N. *Appl. Phys. Lett.* **1992**, *60*, 100.

(6) (a) Ramakrishna, G.; Ghosh, H. N. *Langmuir* **2003**, *19*, 3006. (b) Kamat, P. V.; Huehn, R.; Nicolaescu, R. *J. Phys. Chem. B* **2002**, *106*, 788. (c) Marci, G.; Augugliaro, V.; Lopez-Munoz, M. J.; Martin, C.; Palmisano, L.; Rives, V.; Schiavello, M.; Tilley, R. J. D.; Venezia, A. M. *J. Phys. Chem. B* **2001**, *105*, 1026. (d) Marci, G.; Augugliaro, V.; Lopez-Munoz, M. J.; Martin, C.; Palmisano, L.; Rives, V.; Schiavello, M.; Tilley, R. J. D.; Venezia, A. M. *J. Phys. Chem. B* **2001**, *105*, 1033.

(7) Saito, N.; Haneda, H.; Sekiguchi, T.; Ohashi, N.; Sakaguchi, I.; Koumoto, K. *Adv. Mater*. **2002**, *14*, 418.

(8) Liang, S.; Sheng, H.; Liu, Y.; Hio, Z.; Lu, Y.; Shen, H. *J. Cryst. Growth* **2001**, *225*, 110.

(9) Lee, J. Y.; Choi, Y. S.; Kim, J. H.; Park, M. O.; Im, S. *Thin Solid Films* **2002**, *403*, 533.

(10) Golego, N.; Studenikin, S. A.; Cocivera, M. *J. Electrochem. Soc*. **2000**, *147*, 1592.

(11) Lucas, E.; Decker, S.; Khaleel, A.; Seitz, A.; Fultz, S.; Ponce, A.; Li, W. F.; Carnes, C.; Klabunde, K. J. *Chem. Eur. J.* **2001**, *7*, 2505.

(12) Pan, Z. W.; Dai, Z. R.; Wang, Z. L. *Science* **2001**, *291*, 1947.

(13) (a) Sekar, A.; Kim, S. H.; Umar, A.; Hahn, Y. B. *J. Cryst. Growth* **2005**, *277*, 471. (b) Xu, C. X.; Sun, X. W.; Chen, B. J.; Shum, P.; Li, S.; Hu, X. *J. Appl. Phys*. **2004**, *95*, 661. (c) Meng, X. Q.; Zhao, D. X.; Zhang, J. Y.; Shen, D. Z.; Lu, Y. M.; Liu, Y. C.; Fan, X. W. *Chem. Phys. Lett*. **2005**, *407*, 91. (d) Fan, Z.; Chang, P.-C.; Lu, J. G. *Appl. Phys. Lett*. **2004**, *85*, 6128. (e) Jeong, J. S.; Lee, J. Y.; Cho, J. H.; Lee, C. J.; An, S.-J.; Yi, G.-C.; Gronsky, R. *Nanotechnology* **2005**, *16*, 2455. (f) Xu, C. X.; Sun, X. W.; Dong, Z. L.; Yu, M. B.; My, T. D.; Zhang, X. H.; Chua S. J.; White, T. J. *Nanotechnology* **2004**, *15*, 839. (g) Lee, W.; Jeong, M.-C.; Myoung, J.-M. *Nanotechnology* **2004**, *15*, 1441.

(14) (a) Wu, J. J.; Liu, S. C.; Wu, C. T.; Chen, K. H.; Chen, L. C. *Appl. Phys. Lett*. **2002**, *81*, 1312. (b) Jeong, J. S.; Lee, J. Y.; Cho, J. H.; Suh, H. J.; Lee, C. J. *Chem. Mater.* **2005**, *17*, 2752. (c) Yu, H. D.; Zhang, Z. P.; Han, M. Y.; Hao, X. T.; Zhu, F. R. *J. Am. Chem. Soc.* **2005**, *127*, 2378. (d) Li, Q.; Kumar, V.; Li, Y.; Zhang, H.; Marks, T. J.; Chang, R. P. H. *Chem. Mater.* **2005,** *17*, 1001.

(15) Arnold, M. S.; Avouris, P.; Pan, Z. W.; Wang, Z. L. *J. Phys. Chem. B* **2003**, *107*, 659.

(16) Xu, C. X.; Sun, X. W. *Appl. Phys. Lett.* **2003**, *83*, 3806.

(17) (a) Chik, H.; Liang, J.; Cloutier, S. G.; Kouklin, N.; Xu, J. M. *Appl. Phys. Lett.* **2004**, *84*, 3376. (b) Tang, Q.; Zhou, W. J.; Shen, J. M.; Zhang, W.; Kong, L. F.; Qian, Y. T. *Chem. Commun*. **2004**, 712. (c) Vayssieres, L. *Adv. Mater*. **2003**, *15*, 464. (d) Li, Z. Q.; Ding, Y.; Xiong, Y. J.; Yang, Q.; Xie, Y. *Chem. Eur. J*. **2004**, *10*, 5823. (e) Zhang, Z.; Yu, H.; Shao, X.; Han, M. *Chem. Eur. J*. **2005**, *11*, 3149. (f) Hsu, J. W. P.; Tian, Z. R.; Simmons, N. C.; Matzke, C. M.; Voigt, J. A.; Liu, J. *Nano Lett*. **2005**, *5*, 83. (g) Jie, J.; Wang, G.; Chen, Y.; Han, X.; Wang, Q.; Xu, B. *Appl. Phys. Lett*. **2005**, *86*, 031909. (h) Tak Y.; Yong, K. *J. Phys. Chem. B* **2005**, *109*, 19263.

(18) (a) Park, W. I.; Yi, G.-C.; Kim, M. Y.; Pennycook, S. J. *Adv. Mater*. **2002**, *14*, 1841. (b) Cao, B.; Cai, W.; Duan, G.; Li, Y.; Zhao, Q.; Yu, D. *Nanotechnology* **2005**, *16*, 2567.

(19) (a) Reynolds, D. C.; Look, D. C.; Jogai, B.; Morkoc, H. *Solid State Commun.* **1997**, *101*, 643. (b) Pan, Z. W.; Dai, Z. R.; Wang, Z. L. *Science* **2001**, *291*, 1947. (c) Kong, X. Y.; Wang, Z. L. *Nano Lett.* **2003**, *3*, 1625. (d) Huang, M. H.; Mao, S.; Feick, H.; Yan, H.; Wu, Y.; Kind, H.; Weber, E.; Russo, R.; Yang, P. *Science* **2001**, *292*, 1897. (e) Lao, J. Y.; Wen, J. G.; Ren, Z. F. *Nano Lett.* **2002**, *2*, 1287. (f) Hu, J. Q.; Li, Q.; Meng, X. M.; Lee, C. S.; Lee, S. T. *Chem. Mater*. **2003**, *15*, 305. (g) Wu, J. J.; Liu, S. C. *Adv. Mater.* **2002**, *14*, 215. (h) Xia, Y. N.; Yang, P. D.; Sun, Y. G.; Wu, Y. Y.; Mayers, B.; Gates, B.; Yin, Y. D.; Kim, F.; Yan, H. Q. *Adv. Mater*. **2003**, *15*, 353. (i) Zhang, J.; Sun, L. D.; Yin, J. L.; Su, H. L.; Liao, C. S.; Yan, C. H. *Chem. Mater.* **2002**, *14*, 4172. (j) Peterson, R. B.; Fields, C. L.; Gregg, B. A. *Langmuir* **2004**, *20*, 5114. (k) Liu, B.; Zeng, H. C. *J. Am. Chem. Soc*. **2003**, *125*, 4430. (l) Zhong, X. H.; Knoll, W. *Chem. Commun.* **2005**, 1158. (m) Govender, K.; Boyle, D. S.; Kenway, P. B.; O'Brien, P. *J. Mater. Chem.* **2004**, *14*, 2575 and references therein. (n) Kong, X. Y.; Ding, Y.; Yang, R.; Wang, Z. L. *Science* **2004**, *303*, 1348.

(20) Peng, Y.; Xu, A.-W.; Deng, B.; Antonietti, M.; Coölfen, H. *J. Phys. Chem. B* **2006**, *110*, 2988.

(21) (a) Wang, H.; Xie, C.; Zeng, D.; Yang, Z. *J. Colloid Interface Sci*. **2006**, *297*, 570. (b) Jeong, J. S.; Lee, J. Y.; Cho, J. H.; Suh, H. J.; Lee, C. J. *Chem. Mater*. **2005**, *17*, 2752. (c) Zhang, H.; Yang, D.; Ji, Y.; Ma, X.; Xu, J.; Que, D. *J. Phys. Chem. B* **2004**, *108*, 3955. (d) Zhang, D.-F.; Sun, L.-D.; Yin, J.-L.; Yan, C.-H.; Wang, R.-M. *J. Phys. Chem. B* **2005**, *109*, 8786. (e) Liang, J.; Liu, J.; Xie, Q.; Bai, S.; Yu, W.; Qian, T. *J. Phys. Chem.* B **2005**, *109*, 9463. (f) Shen, G.; Bando, Y.; Lee, C.-J. *J. Phys. Chem. B* **2005**, *109*, 10779.

(22) Mo, M.; Yu, J. C.; Zhang, L.; Li, S.-K. A. *Adv. Mater*. **2005**, *17*, 756.

(23) http://hyperphysics.phy-astr.gsu.edu/hbase/vision/cie.html#c2.

(24) (a) Major, S.; Kumar, S.; Bhatnagar, M.; Chopra, K. L. *Appl. Phys. Lett.* **1986**, *49*, 394. (b) Peng, Y.-Y.; Hsieh, T.-E.; Hsu, C.-H. *Nanotechnology* **2006**, *17*, 174.

(25) Li, W. J.; Shi, E. W.; Zhong, W. Z.; Yin, Z. W. *J. Cryst. Growth* **1999**, *203*, 186.

(26) (a) Dong, L.; Liu, Y. C.; Tong, Y. H.; Xiao, Z. Y.; Zhang, J. Y.; Lu, Y. M.; Shen, D. Z.; Fan, X. W. *J. Colloid Interface Sci*. **2005**, *283*, 380. (b) Seelig, E. W.; Tang, B.; Yamilov, A.; Cao, H.; Chang, R. P. H. *Mater. Chem. Phys*. **2003**, *80*, 257. (c) Oliveira, A. P. A.; Hochepied, J.-F.; Grillon, F.; Berger, M.-H. *Chem. Mater*. **2003**, *15*, 3202. (d) Privman, V.; Goia, D. V.; Park, J.; Matijevic, E. *J. Colloid Interface Sci.* **1999**, *213*, 36. (e) Park, J.; Privman, V.; Matijevic, E. *J. Phys. Chem. B* **2001**, *105*, 11630.

(27) (a) Yin, Y.; Lin, Y.; Xia, Y. *J. Am. Chem. Soc.* **2001**, *123*, 771. (b) Liddell, C. M.; Summers, C. J. *Adv. Mater*. **2003**, *15*, 1715.

(28) Wang, R.-P.; Zhou, G.-W.; Liu, Y.-L.; Pan, S.-H.; Zhang, H.-Z.; Yu, D.-P.; Zhang, Z. *Phys. Rev. B* **2000**, *61*, 16827.

(29) (a) Wang, R. P.; Xu, G.; Jin, P. *Phys. Rev. B* **2004**, *69*, 113303. (b) Callender, R. H.; Sussman, S. S.; Selders, M.; Chang, R. K. *Phys. Rev. B.* **1973**, *7*, 3788. (c) Decremps, F.; Porres, J. P.; Saitta, A. M.; Chervin, J. C.; Polian, A. *Phys. Rev. B* **2002**, *65*, 092101.

(30) Damen, T. C.; Porto, S. P.; Tell, B. *Phys. Rev.* **1966**, *142*, 570.

(31) (a) Xu, C. K.; Xu, G. D.; Liu, Y. K.; Wang, G. H. *Solid State Commun.* **2002**, *122*, 175. (b) Li, Z.; Xiong, Y.; Xie, Y. *Inorg. Chem.* **2003**, *42*, 8105.

(32) (a) Li, Y.; Cheng, G. S.; Zhang, L. D. *J. Mater. Res.* **2000**, *15*, 2305. (b) Vanheusden, K.; Warren, W. L.; Seager, C. H.; Tallant, D. R.; Voigt, J. A.; Gnade, B. E. *J. Appl. Phys.* **1996**, *79*, 7983.

(33) Jin, B. J.; Im, S.; Lee, S. Y. *Thin Solid Films* **2000**, *366*, 107.

(34) Zeng, H.; Cai, W.; Li, Y.; Hu, J.; Liu, P. *J. Phys. Chem. B* **2005**, *109*, 18260.

(35) Zhang, J.; Sun, L. D.; Yin, J. L.; Su, H. L.; Liao, C. S.; Yan, C. H. *Chem. Mater*. **2002**, *14*, 4172.

(36) (a) Hou, H. W.; Xiong, Y. J.; Xie, Y.; Li, Q.; Zhang, J. Y.; Tian, X. B. *J. Solid State Chem.* **2004**, *177*, 176. (b) Wang, Z.; Qian, X. F.; Yin, J.; Zhu, Z. K. *Langmuir* **2004**, *20*, 3441.